Periodica Polytechnica Chemical Engineering, 69(4), pp. 662–672, 2025

Oxalic Acid-assisted Sol–gel Synthesis of High-purity Amorphous Silica from Geothermal Waste

David Candra Birawidha[1,2], Azwar Manaf[2*], Widi Astuti[1**], Amru Daulay[1], Himawan Tri Bayu Murti Petrus[1,3], Nella Astari Ningrum[4], Dwi Asmi[4], Mentari Kirana Nariswari Nariswari[4]

[1] Research Center for Mining Technology, National Research and Innovation Agency (BRIN), Lampung, Gedung B.J. Habibie, Jl. M.H. Thamrin No. 8, Jakarta Pusat 10340, Indonesia
[2] Department of Physics, Faculty of Mathematics and Natural Sciences, Universitas Indonesia, Jl. Lingkar, Pondok Cina, Kecamatan Beji, Kota Depok, Jawa Barat 16424, Indonesia
[3] Department of Chemical Engineering, Faculty of Engineering, Universitas Gadjah Mada, Bulaksumur, Caturtunggal, Kec. Depok, Kabupaten Sleman, Daerah Istimewa Yogyakarta 55281, Indonesia
[4] Department of Physics, Faculty of Mathematics and Natural Sciences, Universitas Lampung, Jl. Prof. Dr. Sumantri Brojonegoro No. 1 Bandar Lampung, 35145, Indonesia
* Corresponding author, e-mail: azwar@sci.ui.ac.id
**Corresponding author, e-mail: widi.mineral@gmail.com

Received: 12 August 2025, Accepted: 03 December 2025, Published online: 16 December 2025

Abstract

This study focuses on the synthesis of amorphous silica from geothermal waste using the sol-gel method with oxalic acid, exploring the impact of pH variation (8 to 13) and the role of microwave heating. Optimal conditions were achieved at pH 8, yielding the highest silica purity of 96.275% and a recovery of 51.16%. Fourier transform infrared analysis confirmed the silica structure, while XRD results verified its amorphous nature with minimal crystalline impurities. Microwave heating significantly enhanced process efficiency by reducing typical carbon residues from gelation. Consistent with previous research, this microwave-assisted approach provides a quantitative improvement, being 30–48 times faster and using 4–50 times fewer reagents while producing nanoparticles as pure, stable, and monodisperse as conventional methods. Field-emission scanning electron microscopy analysis revealed uniform spherical particles under optimal pH, with an average size below 70 nm, whereas extreme pH levels resulted in irregular morphologies. This research contributes to the sustainable utilization of geothermal waste and provides valuable insights for optimizing silica synthesis in various industrial applications.

Keywords

amorphous silica, geothermal waste, sol-gel method, oxalic acid, pH variation, microwave heating

1 Introduction

The development of amorphous silica (SiO_2) materials has made remarkable strides in material science over the past few decades. Thanks to its impressive properties, such as a customizable pore structure, high surface area, and excellent thermal and chemical stability, silica is an ideal material for a wide range of industrial and research applications [1]. The demand for amorphous silica with purity levels up to 99% is driven by its diverse applications, which range from a plant micronutrient and carrier in agriculture, to an absorber in cosmetics, and a key material for manufacturing anodes in the energy industry. However, a key challenge that remains is finding efficient and sustainable synthesis methods that can produce high-purity silica while being environmentally friendly.

The sol-gel method has emerged as a promising technique, allowing precise control over the hydrolysis and condensation reactions of silica precursors [2]. In this process, the choice of catalyst plays a crucial role in determining the reaction speed and the quality of the final product. While strong acids like HCl and H_2SO_4 are typically used for their efficiency, there is a growing interest in using weaker organic acids like oxalic acid due to their safety and sustainability benefits [3].

However, using oxalic acid as a catalyst presents some challenges. It tends to form stable complexes with transition metal cations that act as impurities. These complexes become incorporated into the silica network, and during calcination, they break down and leave carbon residues,

Cite this article as: Birawidha, D. C., Manaf, A., Astuti, W., Daulay, A., Petrus, H. T. B. M., Ningrum, N. A., Asmi, D., Nariswari, M. K. N. "Oxalic Acid-Assisted Sol–Gel Synthesis of High-Purity Amorphous Silica from Geothermal Waste", Periodica Polytechnica Chemical Engineering, 69(4), pp. 662–672, 2025. https://doi.org/10.3311/PPch.41906

making the final silica product less bright and pure [4]. Recent studies by Matinfar and Nychka suggest that controlling the pH in acidic conditions (pH < 7) can help minimize this issue by promoting protonation of the carboxylate group [5]. However, there has been limited research on systems with basic conditions (pH > 7), despite the potential for producing silica with different and interesting morphological properties.

Innovative processes utilizing microwave radiation offer an additional solution to address the issue of carbon residue. The volumetric heating effect caused by dipole-dipole interaction not only improves energy efficiency but also promotes more thorough degradation of organic compounds during the calcination process [6]. Furthermore, from the perspective of the circular economy, which encourages the use of alternative silica sources, particularly from industrial waste, Indonesia, with 40% of the world's geothermal reserves, holds great potential through its geothermal slag waste, which contains amorphous silica with purity reaching 98 wt.% [7, 8].

The role of oxalic acid in sol-gel synthesis has evolved significantly beyond a simple catalyst, as underscored by a growing body of recent literature that highlights its multi-functional capabilities in tailoring the properties of silica-based materials. While traditionally used for pH adjustment, oxalic acid is now recognized as a potent drying control chemical additive (DCCA) and a complexing agent that directly influences the microstructure of the final product. For instance, in the synthesis of sodium silicate based aerogels, oxalic acid was shown to modulate gelation kinetics and pore structure, yielding materials with high specific surface areas and low densities, with its optimal functionality being highly concentration-dependent [4]. Furthermore, its application as a gelling agent in the extraction of silica from geothermal waste and beach sand has proven to be an effective and more environmentally friendly alternative to strong mineral acids. This approach not only successfully produces high-purity silica but also demonstrates advantages in cost-efficiency and reduced environmental impact [9, 10].

The selection of the pH range of 8–13 in this reserach was based on a combination of theoretical rationale and insights from previous literature that highlighted a significant knowledge gap. While it is an established consensus that high-pH conditions generally impair silica purity by increasing silica solubility and facilitating the precipitation of metallic impurities [11–13], this study specifically aimed to investigate the relatively underexplored oxalate-alkali system. The core novelty lies in leveraging the dual functionality of oxalic acid as a complexing and catalytic agent within an alkaline sol-gel environment (pH > 7), an approach rarely documented in previous studies. This investigation was crucial because recent literature underscores the challenges of alkaline synthesis: Mulmeyda et al. corroborate that extreme alkalinity elevates metallic impurities like Fe_2O_3 [11], Jiang et al. documented the formation of carbon residues and Si–C bonds at pH > 11 with organic catalysts [12], and AlMohaimadi et al. revealed that strong alkalis compromise the stability of metal-impurity complexes [13]. By systematically testing pH 8–13, we sought to determine the operational window where the complexing power of oxalate could overcome these typical alkaline drawbacks by integrating the sol-gel method with microwave assistance and the research also aims to determine how this combination can enhance the quality of products derived from local geothermal waste.

2 Materials and methods

2.1 Material and characterisation test

Geothermal silica slag was sourced from PT Geo Dipa Dieng (Central Java, Indonesia). Analytical-grade reagents like NaOH, oxalic acid and methanol were purchased from Supelco, Germany.

The crystalline structure and phase composition of both the initial material and the synthesized amorphous silica were analyzed using X-ray diffraction (XRD) with a Cu-Kα radiation source on a Panalytical X'Pert 3 Powder system from Netherlands, operating at 40 kV and 30 mA. At the same time, the chemical composition of the materials was assessed using X-ray fluorescence (XRF) on an Epsilon 4 XRF Spectrometer from Malvern Panalytical, running at 50 kV and 3 mA from Netherlands.

To identify functional groups and molecular interactions in the samples, Fourier-transform infrared spectroscopy (FTIR) was conducted using a Bruker Invenio R spectrometer from Germany. Additionally, the morphological characteristics of the amorphous silica were observed through field-emission scanning electron microscopy (FESEM) on a Thermo Scientific Quattro system from US.

2.2 Experimental procedure of geothermal silica slag synthesis

In the initial stage of synthesis, 5.62 g of geothermal slag were reacted with 75 mL of a 10% NaOH solution

in a reactor equipped with a magnetic stirrer. The silica extraction process was carried out at 100 °C with stirring at 240 rpm for 3 h, in accordance with the endothermic reaction equation (ΔH = +136.4 kJ/mol):

$$SiO_2(s) + 2NaOH(aq) \rightarrow Na_2SiO_3(aq) + H_2O(l) \quad (1)$$

The resulting sodium silicate solution was then filtered using Whatman No. 42 filter paper to separate any undissolved solid residues. The next step involved titrating the filtrate with a 5 M oxalic acid solution to control the pH of the system within the range of 8–13. The resulting sample is coded according to the pH used during preparation. Thus, the sample labeled pH 8 refers to the one prepared at pH 8. This process follows the exothermic reaction (ΔH = −294.6 kJ/mol):

$$3Na_2SiO_3(aq) + 2C_2H_2O_4(aq) \rightarrow 2NaHC_2O_4(s) + SiO_2(s) + H_2O(l) \quad (2)$$

The formation of the silica gel was observed during the titration process. The resulting gel was then separated by centrifugation at 4000 rpm for 10 min, followed by repeated washing with a methanol-water solution (10 %v) until a neutral pH was reached. The gel product was then dried in an oven at 100 °C for 1 h.

For further optimization, thermal treatment was applied progressively using microwave heating with increasing power levels: 200 W (5 min), 400 W (5 min), 600 W (5 min), and 900 W (5 min). Based on Freitas et al., the microwave-assisted synthesis achieves significant quantitative enhancements, accelerating the reaction by 30–48 times, reducing costs by 18-fold, and lowering reagent use by 4–50 times, all while yielding nanoparticles with comparable or superior purity, stability, and monodispersity to those produced by conventional methods [6]. More details on the heating mechanism, microwave heating was carried out using a domestic microwave oven operating at a frequency of 2.45 GHz with an applied power of 900 W. The treatment was performed on the dried gel to promote uniform heating and prevent excessive foaming during solvent evaporation. The duration of exposure was adjusted based on the desired degree of dehydration and precursor transformation. The final product was comprehensively characterized, including element composition analysis (XRF), crystal structure (XRD), functional groups (FTIR), and surface morphology (FESEM), to assess the quality of the produced amorphous silica material. A brief illustration of the research procedure is presented in Fig. 1.

3 Results and discussion

3.1 Silica characterization with X-ray fluorescence

The XRF analysis results (Table 1) revealed that SiO_2 is the dominant component in all silica samples synthesized using the oxalic acid-based sol-gel process. The quantitative data show a significant purity level, with the highest

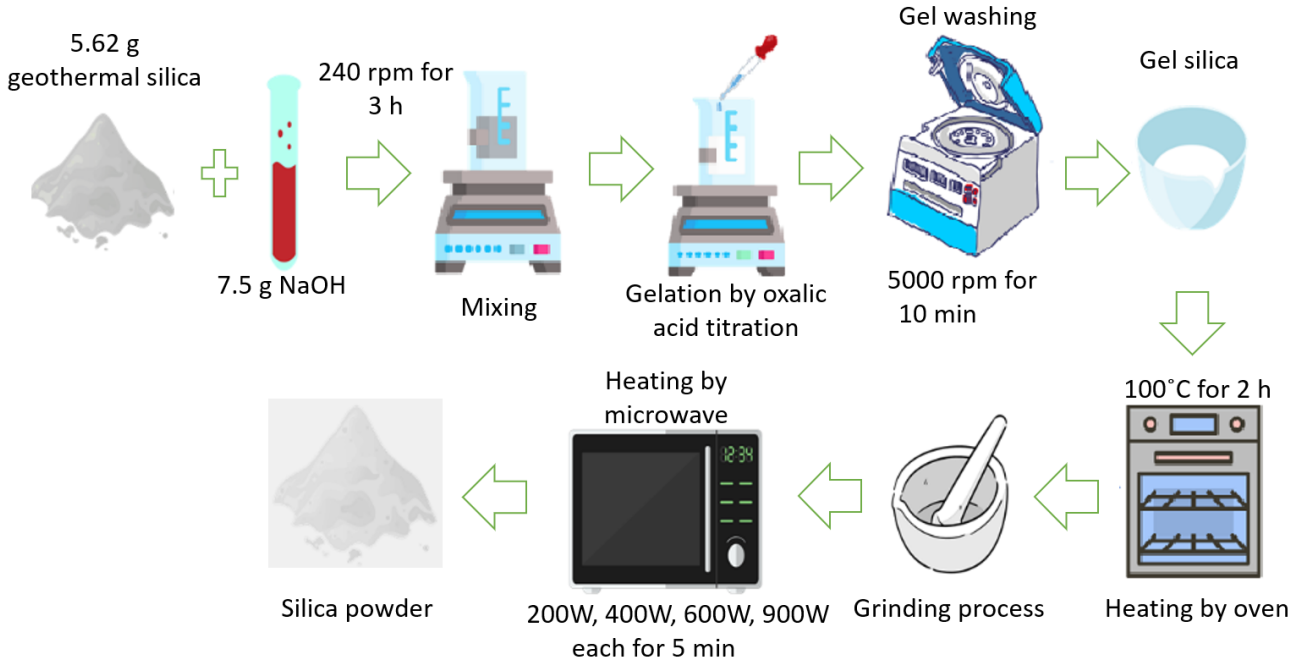

Fig. 1 Illustration of the preparation of amorphous silica from geothermal slag by sol-gel process

Table 1 Composition of the silica sample prepared by the oxalic acid-assisted sol–gel method, characterized by XRF

Oxide	Composition (%wt)						
	Raw geothermal	pH 8	pH 9	pH 10	pH 11	pH 12	pH 13
MgO	-	-	-	-	-	-	0.593 ± 0.540
Al_2O_3	-	0.988 ± 1.381	1.128 ± 0.679	0.790± 0.513	1.271 ± 1.003	0.794 ± 0.863	0.729 ± 0.583
SiO_2	73.240 ± 0.525	96.275 ± 0.595	95.693 ± 0.529	95.641 ± 0.524	94.161 ± 0.562	76.289 ± 0.540	71.820± 0.514
P_2O_5	0.683 ± 0.0512	0.737 ± 0.0758	0.743 ± 0.0741	0.687 ± 0.0960	0.564 ± 0.1087	0.839 ± 0.0518	0.677 ± 0.0870
K2O	3.031 ± 0.612	-	-	-	0.101 ± 0.507	0.149 ± 1.657	0.230 ± 1.036
CaO	1.336 ± 0.564	0.239 ± 1.074	0.246 ± 0.959	0.323 ± 0.818	0.336 ± 0.517	0.909 ± 0.776	1.531 ± 0.691
MnO	-	-	-	-	-	-	0.156 ± 0.586
Fe_2O_3	1.589 ± 0.518	0.474 ± 0.780	0.406 ± 0.689	0.489 ± 0.565	0.611 ± 0.541	3.728 ± 0.653	6.727 ± 0.932
CuO	-	-	-	-	0.175 ± 1.082	0.339 ± 0.503	0.543 ± 1.127
ZnO	0.126 ± 1.349	0.942 ± 0.666	1.140± 0.504	1.302 ± 0.628	1.910± 0.558	11.071 ± 0.552	11.610 ± 0.580
PbO	0.137 ± 1.551	0.275 ± 0.792	0.508 ± 0.639	0.570 ± 0.508	0.783 ± 0.563	5.163 ± 0.526	5.234 ± 0.506
SnO_2	-	-	-	-	-	0.479 ± 0.976	-
Cl_2	19.078 ± 0.514	-	-	-	-	-	-

purity reaching 96.27% at pH 8, followed by pH 9 (95.69%) and pH 10 (95.64%). This pattern suggests that a weakly alkaline to neutral pH range (pH 8–10) is optimal for producing high-purity silica from geothermal raw materials. These findings align with research by Birawidha et al, which reported that conditions near neutral pH tend to produce silica particles with high purity and a more uniform particle size distribution [7].

The silica purification mechanism in this system involves the dual role of oxalic acid as both a complexing agent and a morphology controller. At neutral to weakly alkaline pH levels, the carboxyl groups of oxalic acid form stable complexes with metal cations such as Fe^{2+}, Zn^{2+}, and Ca^{2+} [9, 14]. This interaction effectively prevents the incorporation of these metal impurities into the silica matrix during the precipitation process. Additionally, oxalic acid acts as a reaction rate modulator by selectively binding with silanol (Si-OH), leading to a more controlled and uniform condensation rate. These characteristics explain the system's ability to produce silica particles with high purity and well-defined morphology.

The analysis results in Table 1 show a significant decrease in SiO_2 content under high pH conditions, with values reaching 76.28% at pH 12 and 71.82% at pH 13. This decrease in purity is accompanied by an increase in heavy metal impurities, such as Fe_2O_3 (6.72%), ZnO (11.61%), and PbO (5.23%). This phenomenon suggests that strong alkaline conditions disrupt the silica formation process by destabilizing metal ion complexes and increasing the solubility of silica species in the alkaline medium. At high pH, metal ions tend to form insoluble hydroxides, which become incorporated into the silica gel matrix [15]. The increased levels of Fe, Zn, and Pb impurities at higher pH can be attributed to the formation of soluble hydroxo-complexes, such as $[Fe(OH)_4]^-$, $[Zn(OH)_3]^-$, and $[Pb(OH)_3]^-$, which become more stable in strongly alkaline media. These species remain partially dissolved rather than precipitating, leading to their incorporation or adsorption on the product surface during subsequent processing. Additionally, high pH conditions can alter the redox potential and surface charge of the system, promoting the retention of trace metallic species [16]. The fluctuating Al_2O_3 content (0.79%–1.27%) indicates the stability of aluminosilicate compounds under alkaline conditions. Meanwhile, the presence of small amounts of K_2O suggests the trapping of alkali salts within the silica structure, particularly at extreme pH levels [17].

Heavy metals like Fe, Zn, and Pb tend to precipitate or become trapped within the silica gel when the pH exceeds the isoelectric point of silica (>pH 7–8) [4, 18]. This mechanism explains the sharp decline in SiO_2 purity under strong alkaline conditions, as these metals precipitate into the silica matrix. Based on these findings, it is clear that a pH range of 8–10 is optimal for synthesizing silica with high purity and minimal impurities. At extreme pH levels (>11), the quality of the product decreases due to various impurity incorporation mechanisms. In addition to pH control, the use of microwave heating in sol-gel synthesis has been shown to improve the pore structure of silica [19, 20], offering a solution to enhance material characteristics across different pH conditions.

The experimental data presented in Table 2 reveals the optimal performance of the silica synthesis process at pH 8. Calculation of silica recovery percentage using initial geothermal raw silica mass of 5.62 g and initial SiO_2 composition of 73.24% (Table 1). Under these conditions, the system achieves two important parameters: the highest SiO_2 content of 96.27% and the maximum recovery percentage of 51.16%. Additionally, within the pH range close to neutral, the recovery percentage remains relatively consistent, ranging between 35–40%, with silica purity around 95%, as shown in Table 2. These values indicate that a mildly acidic pH environment, which is not too alkaline, creates ideal conditions for oxalic acid to function as both a complexing agent and a reaction controller.

The effectiveness of the process at pH 8 can be explained through the equilibrium reaction mechanism. Oxalic acid ($C_2H_2O_4$) reaches its optimal condition, where its carboxyl groups form stable complexes with metal ion impurities while maintaining a controlled silica condensation reaction rate. This results in a high-purity product while minimizing material loss during the synthesis process.

The recovery percentage was calculated using the formula shown in Eq. (3).

$$\%\text{Recovery} = \left[\frac{M2\times\%m2}{M1\times\%m1}\right]\times 100\% \quad (3)$$

In this case, % Recovery represents the percentage of the target element recovery, $M1$ is the initial sample mass, % $m1$ is the initial content percentage of the target element, $M2$ is the final sample mass, and % $m2$ is the final content percentage of the target element.

3.2 Silica characterization with Fourier transform infrared spectroscopy

The FTIR analysis results shown in Fig. 2 and Table 3 which is summarize of the main band, provide strong evidence of the formation of amorphous silica from geothermal waste using the sol-gel method with oxalic acid as a catalyst. The spectrum reveals characteristic absorption bands at 1060 cm^{-1} and 790 cm^{-1}, representing the asymmetric and symmetric stretching vibrations of the Si–O–Si bond. According to Guo et al, these bands are key indicators of the formation of the three-dimensional siloxane network, which forms the backbone of the silica structure [21].

An additional band around 950 cm^{-1}, associated with the silanol (Si–OH) group, shows decreasing intensity as the pH increases. This phenomenon, as reported by AlMohaimadi et al., suggests that alkaline conditions promote more efficient condensation reactions between silanol groups, thereby reducing the number of free silanol groups and enhancing the formation of siloxane bridges [13]. A more detailed analysis by Capeletti

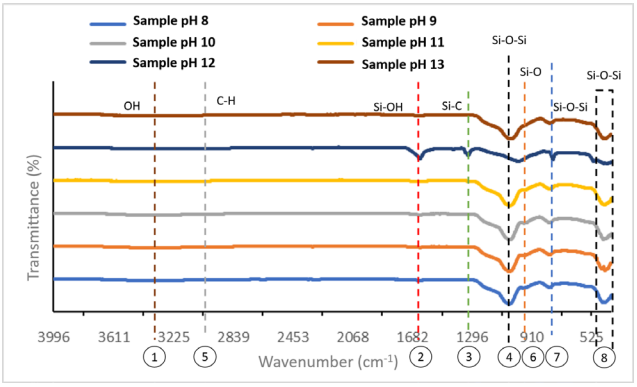

Fig. 2 FTIR characterization of silica synthesized using oxalic acid through sol-gel method

Table 3 Summary of functional groups and their wavenumbers in the synthesized silica at various pH levels

No	Functional group	Wavenumber (cm^{-1}) at various pH					
		8	9	10	11	12	13
1	Si–OH	3412	3410	3404	3443	3411	3400
2	Si–OH	1630	1636	1635	1639	1636	1635
3	Si–C	-	-	-	1318	1330	1330
4	Si–O–Si	1062	1061	1060	1062	1061	1060
5	C–H	-	-	-	2879	2900	2980
6	Si–O	950	951	952	953	951	950
7	Si–O–Si	798	797	799	798	799	798
8	Si–O–Si	469	470	471	469	470	469

Table 2 Calculation of silica recovery obtained from oxalic acid-assisted sol-gel synthesis

No	Sample	Final mass of the sample (g)	Final SiO_2%	% recovery
1	pH 8	2.19	96.27 ± 0.61	51.16 ± 0.57
2	pH 9	2.06	95.69 ± 0.76	47.83 ± 0.63
3	pH 10	1.61	95.64 ± 0.64	37.36 ± 1.02
4	pH 11	1.93	94.16 ± 0.59	44.11 ± 0.51
5	pH 12	1.30	76.28 ± 0.67	24.06 ± 0.56
6	pH 13	0.16	71.82 ± 0.63	2.78 ± 0.65

and Zimnoch further supports these findings, showing a linear correlation between the decrease in silanol band intensity and the increase in the Si–O–Si/Si–OH ratio, which serves as an indicator of progress in the condensation reaction [22]. The spectrum also reveals the presence of water bands at 1630 cm^{-1} (H–O–H bending vibration) and 3400 cm^{-1} (O–H stretching vibration), indicating the adsorption of water molecules within the gel pores. Interestingly, at pH levels above 11, a new band appeared in the 1318–1330 cm^{-1} range, signaling the formation of Si–C bonds, as observed by Lee et al. [23]. This band is likely due to carbon residues from the incomplete degradation of oxalic acid during calcination.

The bands in the 470–525 cm^{-1} range, associated with Si–O–-Si bond vibrations, provide additional insights into the material's structure. According to Nah et al., the relatively weak intensity of these bands confirms the amorphous nature of the silica and offers indications of the degree of regularity in the gel network [24]. Overall, the FTIR characterization results suggest that the pH range of 8–10 is optimal for producing amorphous silica with a well-ordered structure and minimal impurities, as also emphasized by Yuan et al. and Freitas et al. [6, 25]. Jiang et al. further note that strict control of both pH and calcination temperature is crucial to avoid the formation of unwanted Si–C bonds which usually accompanied with C–H bond in 2800–3000 cm^{-1}, particularly when using organic acids as catalysts in silica synthesis [12]. Oxalic acid itself serves a dual function in the synthesis process. As a complexing agent, oxalic acid coordinates with metal ions (e.g., Si or other precursors) through its carboxylate groups, regulating the rate of hydrolysis and condensation reactions. This controlled complexation minimizes premature gelation and leads to a more homogeneous network formation.

Meanwhile, as a catalytic agent, oxalic acid promotes partial proton transfer and facilitates the esterification–hydrolysis equilibrium, accelerating the polycondensation of silanol groups. The synergistic action of these two functions results in a silica matrix with enhanced structural uniformity and reduced defect density. Consequently, the obtained material exhibits improved textural and morphological characteristics.

3.3 Silica characterization with X-ray diffraction

The XRD characterization results presented in Fig. 3 and Table 4, provide a comprehensive overview of the structural transformation that occurs during the synthesis of silica from geothermal slag. The diffraction pattern of the initial material shows clear crystalline characteristics, with sharp peaks identified as NaCl (●) at 2θ positions of 31.6°, 45.4°, 56.4°, 66.2°, 75.2° and 83.9° (COD 96-900-6375), as well as potassium (▲) at 28.3° and 40.5° (COD 96-900-3135), which complete information on the interpretation of this XRD can be seen in the Table 4. According

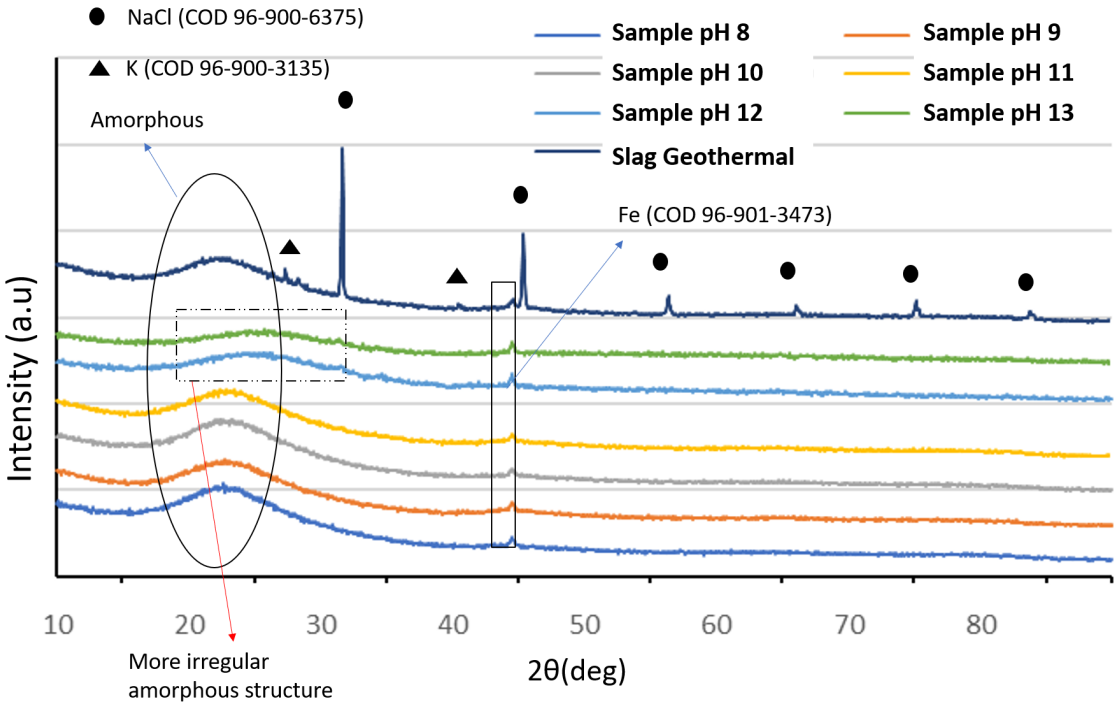

Fig. 3 XRD pattern of silica synthesized via oxalic acid-assisted sol-gel method

Table 4 Summary of phases and corresponding 2θ values of silica synthesized via the oxalic acid-assisted sol–gel method

Reference / COD number	2θ(deg) / hkl					
NaCl (96-900-6375)	31.6 (020)	45.4 (022)	56.4 (222)	66.2 (040)	75.2 (042)	83.9 (242)
K (96-900-3135)	28.3 (020)	40.5 (022)				
Fe (96-901-3473)	45.4 (011)					
Amorphous [27]	20–25 (hump shape)					

to Syabani et al., the presence of these alkali-metal compounds is a hallmark of geothermal slag, and their removal is necessary to obtain silica with high purity [26].

The sol-gel process using oxalic acid as a catalyst successfully maintained the initial crystalline structure, keeping it in the amorphous phase, as shown by the flatter and broader diffraction patterns in the 20°–25° range across all samples. Faustova and Slizhov explained that this diffraction pattern is a key characteristic of amorphous silica, where no sharp peaks are observed, indicating a lack of crystalline order [27]. However, a more detailed analysis revealed that under extreme pH conditions (12–13), small peaks around 45–50° became more apparent, corresponding to the Fe pattern (COD 96-901-3473). Mulmeyda et al. linked this phenomenon to the increased solubility of metal ions under strong alkaline conditions, making their complete elimination difficult during the washing process [11]. The Fe impurities were detected across all pH variations, but as the pH approached neutral, the intensity of the peaks decreased.

Several studies have noted that the presence of heavy metal residues, such as Fe, in the silica matrix often originates from heavy minerals in the geothermal raw material, which are difficult to eliminate through conventional washing methods [11, 28]. The most optimal diffraction pattern was observed in the pH range of 8–10, where the spectrum profile clearly showed the amorphous characteristics without any impurity peaks. These findings are consistent with the research by Dhaneswara et al., who stated that neutral pH conditions provide an ideal balance between hydrolysis and condensation rates, resulting in amorphous silica with high purity [29].

Interestingly, the spectra at pH 12 and 13 displayed a lower intensity (shifting hump) of the amorphous hump compared to other pH levels, suggesting a higher level of atomic disorder in the silica structure formed [30]. Qualitatively, the broader and lower intensity XRD hump observed at pH 12 and 13 compared to samples from pH 8–11 indicates a fundamental difference in their internal structure. The broader hump in the pH 12 and 13 samples signifies a higher degree of amorphous, where the atomic arrangement is more disordered and maintains regularity only over very short distances. Meanwhile, the lower hump intensity suggests that this material has a lower density or a suboptimal degree of condensation in the Si–O–Si network, likely due to higher porosity or a greater abundance of uncondensed silanol (Si–OH) groups. In other words, the samples at pH 12 and 13 are more amorphous and less dense, whereas the samples from pH 8–11 possess a slightly more ordered structure (approaching crystallinity on a very local scale) and are more condensed, as reflected in their narrower and sharper hump.

Based on the XRD analysis in Fig. 3, all silica samples synthesized across the pH range of 8 to 13 were predominantly amorphous. This is evidenced by the low and consistent crystallinity index values, specifically 8.22%, 8.4%, 8.9%, 8.33%, 8.58%, and 7.05%, respectively. These values were calculated by comparing the integrated area of the crystalline peaks to the total area of the XRD diffractogram. The results confirm that over 91% of the formed material is amorphous silica, aligning with the objective of the sol-gel synthesis. The minor crystalline peaks observed were identified as iron impurity phases, consistently appearing across the entire pH range. This finding indicates that the measured crystallinity originates not from the silica itself, but from crystalline iron contaminants potentially derived from the geothermal waste precursor. In summary, the XRD characterization results confirm that oxalic acid is an effective catalyst for producing amorphous silica from geothermal slag, with the pH range of 8–10 proving to be optimal for minimizing crystalline impurities and obtaining a homogeneous amorphous structure.

3.4 Silica characterization with field-emission scanning electron microscopy

Fig. 4 reveals an interesting morphological transformation in the silica particles synthesized from geothermal waste using the oxalic acid-based sol-gel method. In the pH range of 8–9, SEM micrographs show the formation of spherical particles with a homogeneous size distribution and minimal agglomeration. This characteristic reflects a controlled reaction environment, where nucleation and particle growth occur in balance. However, as the pH shifted

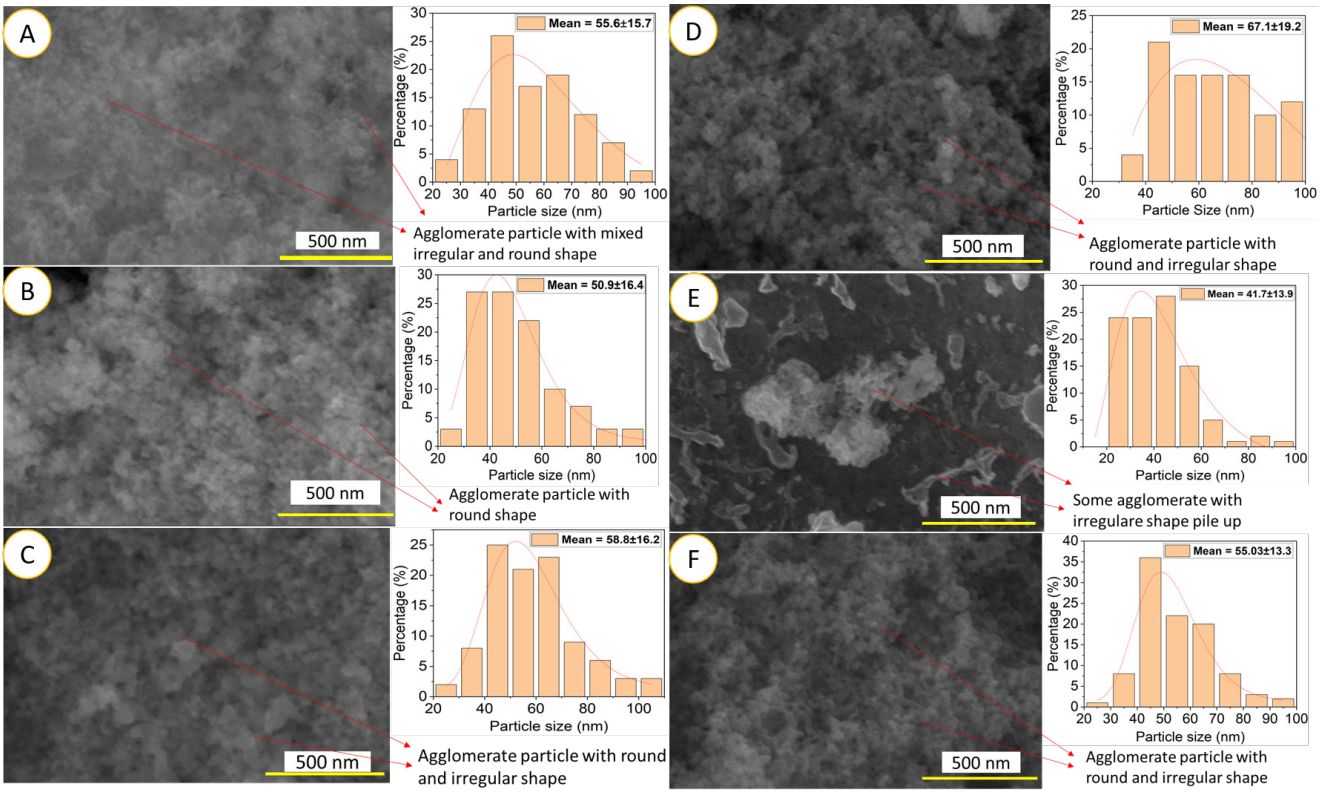

Fig. 4 SEM micrographs and corresponding particle size distribution histograms of silica synthesized at pH: (a) 8, (b) 9, (c) 10, (d) 11, (e) 12, and (f) 13

towards alkaline conditions (10–13), there was a drastic change in particle morphology, leading to the development of irregular structures with a tendency to form stacked aggregates and fine fragments. This morphological shift indicates an acceleration in the condensation reaction kinetics in the strong alkaline medium, as explained by Widiyandari et al., where high pH conditions promote the uncontrolled growth of anisotropic particles [31].

Several key factors have been identified as influencing the morphological evolution of the silica particles. One of these is the dynamics of the chemical reaction. According to Faustova and Slizhov, an exponential increase in pH speeds up the hydrolysis and condensation stages of the silica precursor, which shortens the optimal time needed to form spherical particles [27]. Due to the complexation effect of oxalic acid, it acts as both a catalyst and a complexing agent for transition metal ions (Fe, Al, Ca) from the geothermal raw materials. This complexation process helps prevent the formation of secondary particles that could disrupt the primary nucleation. Additionally, from a mechanical processing standpoint, a study by Petsong et al. confirmed that the uniformity of stirring significantly impacts the final particle size and pore distribution, with more intensive stirring leading to smaller, more spherical particles [32]. Quantitative analysis using ImageJ software on the SEM micrographs revealed that the dominant particle size distribution was below 70 nm at the optimal pH range (8–10), indicating the formation of nanosilica with a relatively controlled and uniform morphology.

Based on Fig. 5, the darker color of the final silica product became more intense at higher pH levels, correlating with the transition metal residues (Fe, Zn, Mn, Pb) incorporated during the rapid condensation process in the alkaline medium. Kunc et al. explained that under extreme alkaline conditions, the excessively fast reaction kinetics hinder the purification of metal ions through conventional washing mechanisms [33]. These results comprehensively indicate that the pH range of 8–10 creates the ideal conditions for synthesizing spherical nanosilica with a narrow particle size distribution.

The role of oxalic acid as a morphology modulator is significantly impactful through the metal complexation mechanism. This finding aligns with the fundamental principles of colloidal particle formation in sol-gel systems, while also providing operational guidance for synthesizing silica materials based on geothermal resources. Also compared with other weak-acid systems commonly employed in sol–gel synthesis, such as citric acid and acetic acid [29, 34], oxalic acid exhibits a stronger chelating capability due to its bidentate carboxylate groups and relatively higher acidity

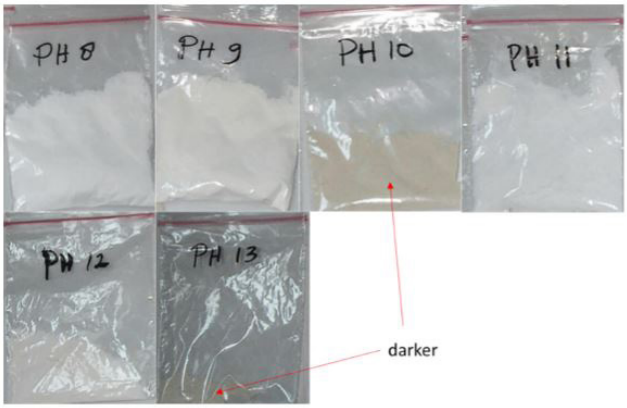

Fig. 5 Visual color change of the samples across pH 8 to 13

(pK_{a1} = 1.25). While citric acid provides mild complexation and promotes gradual gelation, oxalic acid enables tighter coordination with metal centers, leading to better control over hydrolysis and condensation rates. In contrast, acetic acid being weaker and monocarboxylic acts primarily as a pH adjuster rather than a true complexing agent. These differences explain why the oxalic acid system yields a more uniform silica network with fewer structural defects and enhanced textural stability.

4 Conclusions

This study successfully developed a method for producing high-purity amorphous silica from geothermal waste using an oxalic acid-assisted sol-gel process. Under the optimized condition of pH 8, the synthesized silica achieved a purity of 96.3% and a recovery yield of 51%, confirming the efficiency of this route. These quantitative results demonstrate that the use of oxalic acid not only improves the structural homogeneity of silica but also enhances its production efficiency. A key innovation was the integration of microwave heating, which significantly improved the synthesis by providing more uniform heat distribution, accelerating the reaction time, and reducing carbon residues typically formed during gelation.

Comprehensive characterization using XRF, FTIR, and XRD confirmed the high purity and amorphous nature of the silica, while SEM analysis revealed well-formed and uniformly sized particles at the optimal pH, contrasting with the irregular morphologies observed at extreme pH levels. Overall, the findings provide both a mechanistic understanding and a practical pathway for obtaining high-quality silica. This research highlights the potential of combining microwave-assisted sol-gel processing with oxalic acid as a sustainable and efficient strategy for valorizing geothermal waste into a valuable material.

Acknowledgement

The authors acknowledge the facilities, scientific and technical support from Minerals Laboratory Lampung, National Research and Innovation Agency through E-Layanan Sains, Badan Riset dan Inovasi Nasional (BRIN). This research also supported by Research Organization for Nanotechnology and Materials BRIN through Rumah program funding research in 2025. We also thank you for the support from Department of Physics, Faculty of Mathematics and Natural Sciences, Universitas Indonesia as part of the "Hibah Publikasi Pascasarjana FMIPA UI 2025-2026" program under contract number PKS-34/UN2.F3.D/PPM.00.02/2025.

References

[1] Jenie, S. N. A., Ghaisani, A., Ningrum, Y. P., Kristiani, A., Aulia, F., Petrus, H. T. M. B. "Preparation of silica nanoparticles from geothermal sludge via sol-gel method", AIP Conference Proceedings, 2026(1), 020008, 2018. https://doi.org/10.1063/1.5064968

[2] Jiang, B., Xia, D., Yu, B., Xiong, R., Ao, W., Zhang, P., Cong, L. "An environment-friendly process for limestone calcination with CO_2 looping and recovery", Journal of Cleaner Production, 240, 118147, 2019. https://doi.org/10.1016/j.jclepro.2019.118147

[3] Maseko, N. N., Enke, D., Iwarere, S. A., Oluwafemi, O. S., J. Pocock, J. "Synthesis of Low Density and High Purity Silica Xerogels from South African Sugarcane Leaves without the Usage of a Surfactant", Sustainability, 15(5), 4626, 2023. https://doi.org/10.3390/su15054626

[4] Al-Mothafer, Z. H., Abdulmajeed, I., Al-Sharuee, I. "Effect Of Oxalic Acid As A Catalyst And Dry Control Chemical Additive (DCCA) For Hydrophilic Aerogel Base Sodium Silicate By Ambient Pressure Drying", Journal of Ovonic Research, 17(2), pp. 175–183, 2021.

[5] Matinfar, M., Nychka, J. A. "Process Mapping of the Sol–Gel Transition in Acid-Initiated Sodium Silicate Solutions", Gels, 10(10), 673, 2024. https://doi.org/10.3390/gels10100673

[6] Freitas, D. C., Mazali, O., Sigoli, A., Francischini, S., Aur, M., Arruda, Z. "The microwave-assisted synthesis of silica nanoparticles and their applications in a soy plant culture", RSC Advances, 13(39), pp. 27648–27656, 2023. https://doi.org/10.1039/d3ra05648a

[7] Birawidha, D. C., Manaf, A., Astuti, W., Dualay, A., Haryono, T., Sari, Y., Suprihatin, S. "Eco Friendly Citric Acid-Assisted Sol-Gel Synthesis of High- Purity Nano Silica from Dieng Geothermal Slag: Characterization and Optimization Method", Indonesian Physical Review, 8(2), pp. 530–539, 2025. https://doi.org/10.29303/ipr.v8i2.486

[8] Sujoto V. S. H.., Tangkas, I. W. C. W. H., Astuti, W., Sumardi, S., Jenie, S. N. A., Tampubolon, A. P. C., Syamsumin, S., Utama, A. P., Petrus, H. T. B. M., Kusumastuti, Y. "Penentuan kondisi optimum pembuatan silica gel menggunakan silika geothermal dengan metode sol-gel", Jurnal Rekayasa Proses, 17(2), pp. 122–128, 2023. https://doi.org/10.22146/jrekpros.77696

[9] Sumari, S., Asrori, M. R., Prakasa, Y. F., Baharintasari, D. R. "Silica extract from Malang beach sand via leaching and sol-gel methods", International Journal of Advances in Applied Sciences, 12(1), pp. 74–81, 2023. https://doi.org/10.11591/ijaas.v12.i1.pp74-81

[10] Ali, A. A., Nassar, M. Y., Shama, S. A., El Sharkwy, A. M., El Sayed, N. E. " Sol-Gel Auto-Combustion Synthesis and Identification of Silicon Dioxide Nanoparticles forThe Removal of Sunset Dye from Aqueous Solutions", Benha Journal of Applied Sciences, 5(7), pp. 217–229, 2020. https://doi.org/10.21608/bjas.2020.227356

[11] Mulmeyda, R., Widakusuma, R. R., Chaerani, S. P., Purwanto, A., Rafsanjani, R. A., Zapar, H. M., Ardhi, B. P. "Synthesis of α-Fe_2O_3 and α-Fe_2O_3/SiO_2 Composite from Geothermal Waste by Sol-Gel Method and Their Characterization", Chemistry and Materials, 4(1), pp. 24–33, 2025. [online] Available at: https://www.researchgate.net/publication/389450811_Synthesis_of_a-Fe2O3_and_a-Fe2O-3SiO2_Composite_from_Geothermal_Waste_by_Sol-Gel_Method_and_Their_Characterization#fullTextFileContent [Accessed: 04 December 2025]

[12] Jiang W., Chen, J., Wu, X., Wu, L., Yi, J., Jiang, Z., Wang, B., Wang, W., Wei, Y., Sun, T. "Simulation of chemical reactions with methanol and oxalic acid on 4H-SiC surfaces before and after nanoabrasion", Applied Surface Science, 677, 161035, 2024. https://doi.org/10.1016/j.apsusc.2024.161035

[13] AlMohaimadi, K. M., Albishri, H. M., Thumayri, K. A., AlSuhaimi, A. O., Mehdar, Y. T. H., Hussein, B. H. M. "Facile Hydrothermal Assisted Basic Catalyzed Sol Gel Synthesis for Mesoporous Silica Nanoparticle from Alkali Silicate Solutions Using Dual Structural Templates", Gels, 10(12), 839, 2024. https://doi.org/10.3390/gels10120839

[14] Feyzi, E., Kumar M R, A., Li, X., Deng, S., Nanda, J., Zaghib, K. "A comprehensive review of silicon anodes for high-energy lithium-ion batteries: Challenges, latest developments, and perspectives", Next Energy, 5, 100176, 2024. https://doi.org/10.1016/j.nxener.2024.100176

[15] De Vasconcelos, A. B. P., Silva, W. E., Belian, M. F. "*pH* dependent drug delivery based on silica xerogel", Journal of the Chilean Chemical Society, 62(4), pp. 3700–3702, 2017. https://doi.org/10.4067/s0717-97072017000403700

[16] Balintova, M., Petrilakova, A. " Study of pH Influence on Selective Precipitation of Heavy Metals from Acid Mine Drainage", Chemical Engineering Transactions, 25, pp. 345–350, 2011. https://doi.org/10.3303/CET1125058

[17] Ibrahim, A. F. M., Seifelnassr, A. A. S., Al-Abady, A., El-Salmawy, M. S., Abdelaal, A. M. "Characterization and Iron Removal Enhancement of El-Zaafarana White Sand", Mining, Metallurgy & Exploration, 39(5), pp. 2187–2198, 2022. https://doi.org/10.1007/s42461-022-00667-0

[18] Danks, A. E., Hall, S. R., Schnepp, Z. "The evolution of 'sol-gel' chemistry as a technique for materials synthesis", Materials Horizons, 3(2), pp. 91–112, 2016. https://doi.org/10.1039/c5mh00260e

[19] González-Lavín, J., Arenillas, A., Rey-Raap, N. "Microwave-Assisted Synthesis of Iron-Based Aerogels with Tailored Textural and Morphological Properties", ACS Applied Nano Materials, 6(19), pp. 18582–18591, 2023. https://doi.org/10.1021/acsanm.3c04173

[20] Mahalingam, V. Sivaraju, M. "Microwave-Assisted Sol-Gel Synthesis of Silica Nanoparticles Using Rice Husk as a Precursor for Corrosion Protection Application", Silicon, 15(4), pp. 1967–1975, 2023. https://doi.org/10.1007/s12633-022-02153-0

[21] Guo, X., Zhang, Q., Ding, X., Shen, Q., Wu, C., Zhang, L., Yang, H. "Synthesis and application of several sol–gel-derived materials via sol–gel process combining with other technologies: a review", Journal of Sol-Gel Science and Technologies, 79(2), pp. 328–358, 2016. https://doi.org/10.1007/s10971-015-3935-6

[22] Capeletti, L. B., Zimnoch, J. H. "Fourier Transform Infrared and Raman Characterization of Silica-Based Materials", In: Stauffer, M. T. (ed.) Applications of Molecular Spectroscopy to Current Research in the Chemical and Biological Sciences, IntechOpen, 2016, pp. 3–22. ISBN 978-953-51-5083-1 https://doi.org/10.5772/64477

[23] Lee, J. H., Kwon, J. H., Lee, J. W., Sun Lee, H., Chang, J. H., Sang, B. I. "Preparation of high purity silica originated from rice husks by chemically removing metallic impurities", Journal of Industrial and Engineering Chemistry, 50, pp. 79–85, 2017. https://doi.org/10.1016/j.jiec.2017.01.033

[24] Nah, H. Y. "Role of oxalic acid in structural formation of sodium silicate-based silica aerogel by ambient pressure drying", Journal of Sol-Gel Science and Technology, 852, pp. 302–310, 2018. https://doi.org/10.1007/s10971-017-4553-2

[25] Yuan, M., Guo, X., Liu, Y., Pang, H. "Si-based materials derived from biomass: Synthesis and applications in electrochemical energy storage", Journal of Materials Chemistry A, 7(39), pp. 22123–22147, 2019. https://doi.org/10.1039/c9ta06934h

[26] Syabani, M. W., Rochmadi, R., Perdana, I., Prasetya, A. "FTIR study on nano-silica synthesized from geothermal sludge", AIP Conference Proceedings, 2440(1), 030014, 2022. https://doi.org/10.1063/5.0075015

[27] Faustova, Z. V., Slizhov, Y. G. "Effect of solution pH on the surface morphology of sol–gel derived silica gel", Inorganic Materials, 53(3), pp. 287–291, 2017. https://doi.org/10.1134/S0020168517030050

[28] Mroczek, E. K., Graham, D., Bacon, L. "Removal of arsenic and silica from geothermal fluid by electrocoagulation", Journal of Environmental Chemical Engineering, 7(4), 103232, 2019. https://doi.org/10.1016/j.jece.2019.103232

[29] Dhaneswara, D., Fatriansyah, J. F., Situmorang, F. W., Haqoh, A. N. "Synthesis of Amorphous Silica from Rice Husk Ash: Comparing HCl and CH3COOH Acidification Methods and Various Alkaline Concentrations", International Journal of Technology (IJTech), 11(1), pp. 200–208, 2020.
https://doi.org/10.14716/ijtech.v11i1.3335

[30] Awadh, S. M., Yaseen, Z. M. "Investigation of silica polymorphs stratified in siliceous geode using FTIR and XRD methods", Materials Chemistry and Physics, 228, pp. 45–50, 2019.
https://doi.org/10.1016/j.matchemphys.2019.02.048

[31] Widiyandari, H., Pardoyo, P., Sartika, J., Putra, O. A., Purwanto, A., Ernawati, L. "Synthesis of Mesoporous Silica Xerogel from Geothermal Sludge using Sulfuric acid as Gelation Agent", International Journal of Engineering Transactions A: Basics, 34(7), pp. 1569–1575, 2021.
https://doi.org/10.5829/IJE.2021.34.07A.02

[32] Petsong, K., Luangchaisri, C., Muangphat, C. "Effect of mixing methods and chemical concentrations on the homogeneity of SiO_2 microsphere via Stöber and modified Stöber methods", ScienceAsia, 51(1), pp. 1–11, 2025.
https://doi.org/10.2306/scienceasia1513-1874.2025.017

[33] Kunc, F., Balhara, V., Sun, Y., Daroszewska, M., Jakubek, Z. J., Hill, M., Brinkmann, A., Johnston, L. J. "Quantification of surface functional groups on silica nanoparticles: Comparison of thermogravimetric analysis and quantitative NMR", Analyst, 144(18), pp. 5589–5599, 2019.
https://doi.org/10.1039/c9an01080g

[34] Nuryono, N., Narsito, N. " Effect of Acid Concentration on Characters of Silica Gel Synthesized from Sodium Silicate", Indonesian Journal of Chemistry, 5(1), pp. 23–30, 2010.
https://doi.org/10.22146/ijc.21834